Childs Nerv Syst (2006) 22: 475–480
DOI 10.1007/s00381-005-0026-y

ORIGINAL PAPER

Shih-Hwa Chiou
Chung-Lan Kao
Han-Tso Lin
Wen-Ser Tseng
Ren-Shyan Liu
Chen-Fun Chung
Hung-Hai Ku
Ching-Po Lin
Tai-Tong Wong

Monitoring the growth effect of xenotransplanted human medulloblastoma in an immunocompromised mouse model using in vitro and ex vivo green fluorescent protein imaging

Received: 1 July 2005
Published online: 16 March 2006

S.-H. Chiou · H.-T. Lin
Department of Education and Research,
The Neurological Institute,
Taiwan, Republic of China

C.-L. Kao
Department of Physical
Medicine & Rehabilitation,
The Neurological Institute,
Taiwan, Republic of China

W.-S. Tseng · T.-T. Wong (✉)
Division of Pediatric Neurosurgery,
The Neurological Institute,
Taipei Veterans General Hospital
and National Yang-Ming University,
Taiwan, Republic of China
e-mail: ttwong@vghtpe.gov.tw
Tel.: +886-2-28757587
Fax: +886-2-28757587

R.-S. Liu
Department of Nuclear Medicine,
Taipei Veterans General Hospital
and National Yang-Ming University,
Taiwan, Republic of China

H.-T. Lin · C.-F. Chung · H.-H. Ku
Institute of Anatomy and Cell Biology,
National Yang-Ming University,
Taiwan, Republic of China

C.-P. Lin
Institute of Neuroscience,
National Yang-Ming University,
Taiwan, Republic of China

S.-H. Chiou
Institute of Clinical Medicine,
National Yang-Ming University,
Taiwan, Republic of China

Abstract *Introduction:* Medulloblastoma (MB) is one of the most common malignant brain tumors in children. It is a radiosensitive tumor. At 5 years after radical surgical excision and craniospinal axis irradiation, the tumor-free survival rate is from 50 to 70% [Halperin EC, Constine LS, Tarbell NJ, Kun LE. Pediatric radiation oncology (2005)]. *Case report:* In this study, we established xenotransplanted human MB (hMB) cells — isochromosome 17q — in a severe combined immunodeficiency (SCID) mouse model. We further transduced green fluorescent protein (GFP) into hMB cells to evaluate these hMB cells grafted in SCID mice. *Results:* The result of an ex vivo GFP imaging system showed that a small lesion of the third-week-hMB-transplanted graft presented "green" signals with a clear tumor margin before any tumor-related symptoms were noted. We also demonstrated that the tumor progression could be monitored by GFP imaging for up to 12 weeks post-transplantation. *Conclusions:* This novel approach of GFP imaging assessment provides more accurate information of tumor status for experimental brain tumor studies. Because MB is sensitive to radiation and also response to chemotherapy, this SCID mouse model will be helpful for preclinical studies in the future.

Keywords Medulloblastoma · Green fluorescent protein imaging · SCID mouse model

Introduction

Medulloblastomas (MB) are malignant posterior fossa tumors which comprise 13–20% of all childhood brain tumors [1–3]. The prognosis of MB patients is based on age, extent of surgical resection, and presence of metastases, but these clinical data are not always sufficient for proper classification and reliable therapy [1–3]. As for the remedy of MB, surgical excision alone is not curative [1, 2]. Virtually all tumors recur and patients die within 3 years without adjuvant treatment [4]. To develop new therapeutic strategies for improving the treatment effects in MB patients, the establishment of both animal models and an accurate evaluation system for in vivo preclinical research is essential.

Preclinical animal models play a critical role in cancer research [5]. However, the limitations of several animal models were reported in the study of pediatric brain tumors

[5, 6]. There is also specific interest in the xenografting of MB/primitive neuroectodermal tumors, because of their relevance to concurrent clinical research and practice [7]. Conventional subcutaneous site heterotransplantation in animal models is the easiest method for monitoring tumor growth [8]. Because of the absence of a blood–brain barrier equivalent and the lack of similarities to the environment of the central nervous system, the effects of therapeutic assays may not be optimal. To imitate and construct an in vivo environment for MB, we firstly cultured a human MB (hMB) (Doay) cell line, and then xenotransplanted these hMB cells into the striatum area of the brains of mice with severe combined immunodeficiency (SCID)—a kind of immunocompromised strain, which can incubate human tissues and cells without the effect of rejection [9]. To further evaluate the proliferation of hMB cells in vitro and in vivo, the gene of green fluorescent protein (GFP) was transduced and integrated into the chromosome of MB cells. Then, these GFP-positive MB cells were xenotransplanted into the stratium of SCID mice and evaluated with the GFP imaging system.

Materials and methods

This research follows the tenets of the Declaration of Helsinki, and was reviewed by the Institutional Review Committee at Taipei Veterans General Hospital. The culture procedure of MB cells was performed as previously described [10]. The hMB (Doay) cell line was purchased from American Type Culture Collection Cell Bank (USA). The suspended cells were washed with phosphate-buffered saline (PBS) (pH 7.2) and treated with 0.025% trypsin-EDTA [Grand Island Biological Company (GIBCO)] in Hank's balanced salt solution (Sigma) for 15 min at 37°C, and then passed through a 30-μm-mesh nylon screen. The filtrate was centrifuged (800×*g*, 5 min) and the resulting cell pellet was seeded into a T75 flask. Cultures were grown in Dulbecco's modified eagle's medium (GIBCO) containing 10% heat-inactivated fetal bovine serum, 2 mM glutamine, penicillin (100 units/ml), and streptomycin (100 μg/ml).

Comparative genomic hybridization (CGH)

The CGH procedure was performed as previously described [10, 11]. Briefly, the slides were aged for 2 days before denaturation at 72°C in 70% spectrum red formamide/2× saline sodium citrate. Nick-translated, spectrum red-labeled tumor DNA and spectrum green-labeled normal DNA were coprecipitated with excess unlabeled human *Cot*-1 DNA (GibcoBRL, USA), denatured, and hybridized to the normal metaphase slide preparations. Ten images were analyzed by a Cytovision workstation.

GFP gene delivery by murine stem cell retroviral vectors (MSCV) retrovirus

The complementary DNA (cDNA) plasmids of MIGFP, PMD, and VZV-G of MSCV (a gift from Shih CC and Yee JK; City of Hope, Duarte, CA, USA) have been described previously [12]. To generate GFP retroviral supernatants, 293 cells were transiently transfected by calcium phosphate-mediated coprecipitation with 5 μg of the plasmids. The cells were fed at 24 h postinfection, and the retroviral supernatant was used at 48 h. The cells continued to produce high-titer retrovirus for another 2 days, and the supernatant was used if needed for additional experiments. The supernatant was collected, brought to 8 μg of polybrene per ml–10 mM 4-2-hydroxyethyl-1-piperazine-ethanesulfonic acid, and filtered 0.45 μm pore-sized filter for use. Stem cells for infection were washed and trypsinized. They then plated at 10^6 cells per well in a six-well dish and were centrifuged. The stem cell medium was removed, and retroviral supernatant was added at 1 ml/10^6 cells.

Ex vivo GFP imaging

The animal experiment follows and obeys the "Principles of laboratory animal care" of Taipei Veterans General Hospital and National Yang-Ming University. Of the MB cells, 2×10^5 were injected into the left striatum of SCID mice (eight w/o), following the previous protocols [10, 13]. The excitation filter of 470 nm with a lamp supply of optical lighting of 150 W (Southern California Services, USA) was used as an excited light source (470 nm) to project on the foci of GFP-positive cells of living mice and ex vivo transplanted tissues. The GFP imaging capture and photography was based on the recordings of a digital camera (Olympus) through the optical configuration of a dissected microscope (SZ60, Olympus) with a 515-nm viewing (emission) filter. The growth size of the xenografts were plotted and analyzed with Image-ProPlus software (Media Cybernetics, USA).

Immunohistochemistry

The 4-μm paraffin sections were deparaffinized in xylene, rehydrated in a series of graded alcohols, and immunostained with antibodies against Synatophysin (ChemMate, DAKO, Glostrup, Denmark), neuron-specific enolase (ChemMate, DAKO), and glial fibrillary acidic protein (ChemMate, DAKO). Immunoreactive signals were detected with a mixture of biotinylated immunoglobulin G (IgG) antibody and peroxidase-conjugated streptavidin (labelled Streptavind-Biotin system, DAKO).

Results

Synatophysin [14] is the most common marker for diagnosing MB in pathohistological review (Fig. 1a). By using immunohistochemisty, the morphology of hMB (Doay) cells presented many small cells with hyperchromatic nuclei which were strongly positive synatophysin (Fig. 1b). This strain of hMB cells (Fig. 1b) could be passed stably for more than 30 passages without loss of growth, viability, or morphological and immunochemical features of the parental tumor cell. To further monitor the tumor cell proliferation in vitro, GFP gene was transduced into hMB cells (Fig. 1c and d) using murine stem cell viral vector. The GFP-positive hMB (hMB-GFP) cells were then sorted by flow cytometry. These hMB-GFP cells could be passaged, and constitutively express GFP in vitro culture (Fig. 1c and d).

The cell doubling time of this strain of hMB cells was 21.5 h, as estimated from an in vitro growth curve (Fig. 2). We analyzed next the chromosomal abnormality of these hMB cells. Giemsa banding results revealed aneuploidy in these cells. Comparative genomic hybridization was used to determine the copy number karyotype, and the results showed gains of chromosome regions on 1p, 1q23, 1q32, 1q41q42, 2p21p23, 3q21, 5q13, 5q31, 6p, 6q12q14, 6q 24q27, 7p, 7q, 9q21q34, 12q22q24.3, 14q21q22, 14q23, 17q, 19p, 19q, 21q22, and 22q13, and losses of chromosome regions on 4q, 8p21p23, 9p21, 10p12p13, 10p 11.2, 10q11.2q21, 10q24, 13p12p13, 13q12q34, 14p, 16q11.2q22, 17p12p13, 18p, 18q, 21p, and 22p11.2p12. Typicalkaryotypic findings, such as isochromosome 17q, in our hMB cells were consistent with previous reports [10, 14, 15].

To early detect and longitudinally evaluate the growth-effect of hMB-GFP cells in living immunocompromised animals, we xenogenically transplanted human hMB cells which constitutively expressed GFP into the striatum of SCID mice. By using a specific GFP detection system, an early, small lesion that expressed "green" signals (1×1 mm) was clearly detected in the coronal section of third-week hMB-GFP-transplanted mice (Fig. 3a and c) before any neurological symptoms were noted. Significant neurological signs were developed in these hMB-transplanted mice 10 weeks after transplantation. At the same time, the ex vivo GFP imaging further monitored the growth of hMB in the tenth-week-transplanted graft (4×5 mm) and precisely traced the tumor's invasion of the corpus callosum and the cortex area (Fig. 3b and d). In comparison to the tumor survey of the MicroPET system (MicroPET R4; CTI Molecular Imaging, Germany), uptake of [^{18}F] fluorodeoxyglucose (FDG) was found in the same mouse at the tenth week, but a significant signal of [^{18}F] FDG could not be identified at the third week. Indeed, the assessment of ex vivo GFP imaging provided a better stereoscopical and anatomical illustration to define the tumor-infiltrated margins than the results of MicroPET (Fig. 3e) and traditional

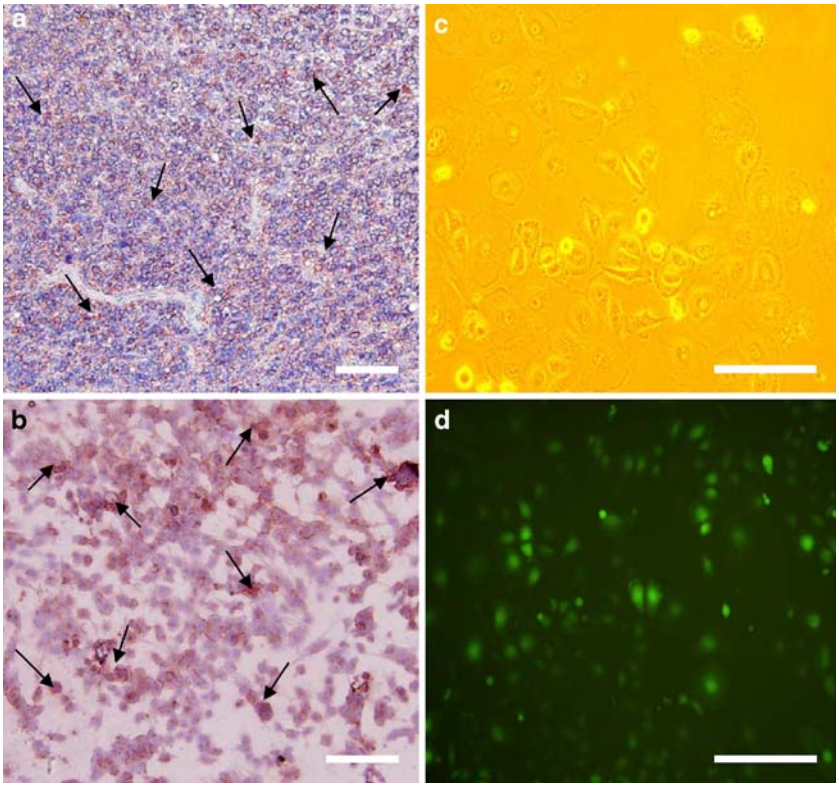

Fig. 1 Isolation and characterization of hMB cells: **a** Detection of the protein expression of synatophysin (*red color*: *arrows*) in the brain tissue of a MB patient. **b** Immunohistochemical study of hMB cell. **c** Phase contrast-hMB cells in vitro. **d** Expression of GFP in hMB cells in vitro

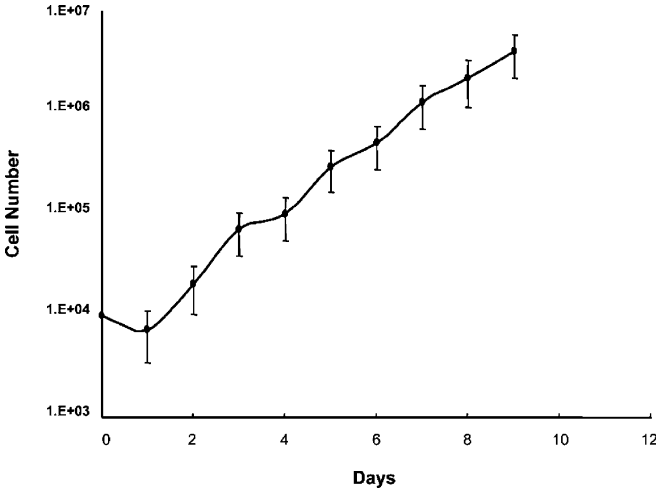

Fig. 2 Cell doubling time of hMB (Doay) cells

histological review (Fig. 4a–d). Furthermore, the median survival time of hMB-transplanted mice was 6.9 weeks (Fig. 4f). The tumor size increased rapidly after 6 weeks post-transplantation (Fig. 4e). This finding is comparable with the median survival time.

Discussion

MBs are the most common posterior fossa tumors in children [1, 2]. As for the adjunctive non-invasive evaluation method, neuroimaging often plays important parts in deciding treatment strategies in MB [16]. Thus, the establishment of an effective monitoring system for tumor proliferation is essential. In this study, we established xenotransplanted hMB cells — isochromosome 17q — in a SCID mouse model. GFP was transduced into hMB cells to evaluate the hMB cells grafted in SCID mice. The ex vivo GFP imaging system revealed a small lesion of a third-week hMB-transplanted graft presenting "green" signals with a clear tumor margin, and the tumor progression could be monitored for up to 12 weeks post-transplantation. These results correlated with tumor stages by pathological sections.

Preclinical animal models play a key role in cancer research [5, 8]. Wetmore et al. have shown that a loss of p53 can enhance the MB-promoting effects of the *PTCH* gene mutation, and the ptc+/−p53−/− mutated mice were generated for a model of MB [17, 18]. However, several mutated genes and the disregulation of protein expressions are also involved in the developmental process and tumorigenesis of MBs [19–22]. For example, a recent study revealed that transcriptional silencing of DLC-1 (a tumor-suppressor gene on chromosome 8p22) through promoter hypermethylation may critically contribute to tumorigenesis in MBs [19]. Furthermore, several target genes including the mutation of the REN^{kctd11} gene, the hypermethylation of the HIC1 gene, and the upregulation of the PDGFRA and PDGFRB genes could also be responsible for the initiation and progression of MBs [20–22]. Thus, to reflect the complicated tumor characters and the individual variations of MB patients, animal models carried out with xenotransplanted hMB cells and grafts would be an alternative strategy for the development of new remedies.

To efficiently and quantitatively evaluate the growth effect of tumor cells in vitro and in vivo, GFP, a fluorescent gene derived from jellyfish [23], was used in this study as an indicator and reporter gene to label and monitor the tumor growth of hMB. Indeed, fluorescent genes and proteins are basic analytical tools used in molecular and cellular applications [23–25]. Fluorescent dyes such as ethidium bromide, SYBR Green I stain, SYPRO Orange I stain, and Nile Red stain are also widely used to efficiently detect trace amounts of DNA, RNA, and protein in molecular biological research [25–27]. We demonstrated in this study the incorporation of GFP reporter genes into the genomes of hMB cells as markers of tumor proliferations and invasions, both in cells and in living animals. Without adding any exogenous substrates or antibodies, the

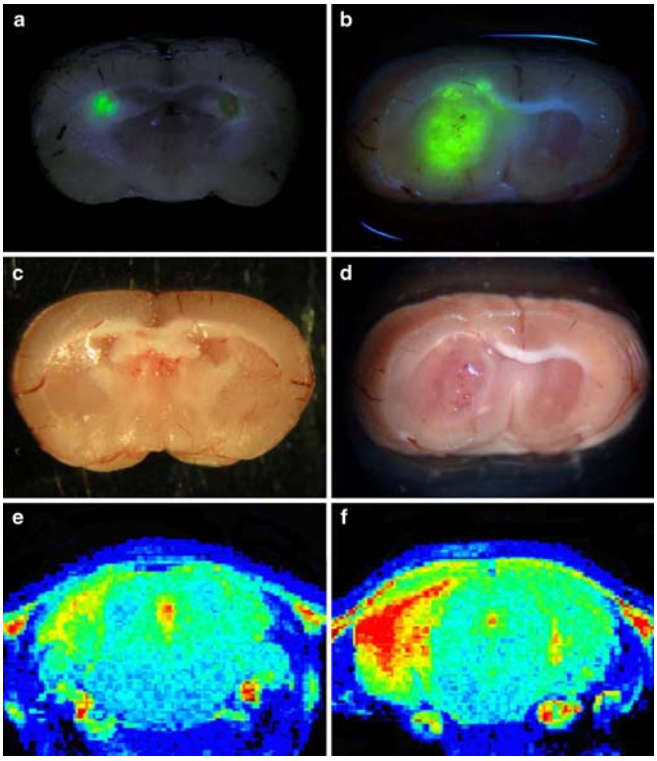

Fig. 3 Analysis of ex vivo GFP imaging in the post-transplanted (p/t) hMB cells of mice: **a** and **c** GFP imaging of third week p/t. **b** and **d** GFP imaging of tenth week p/t. **e** MicroPET imaging of third week p/t. **f** MicroPET imaging of tenth week p/t

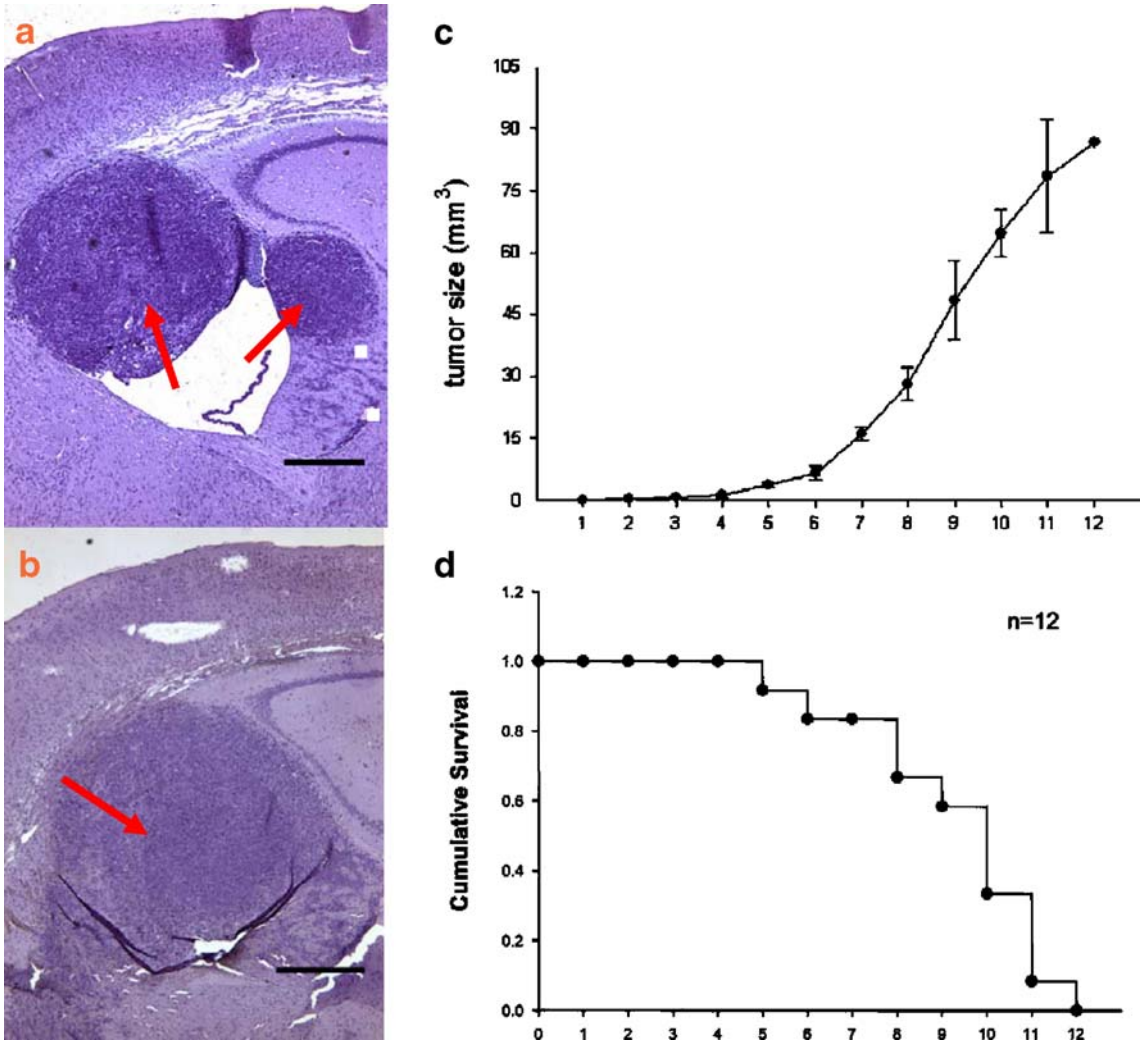

Fig. 4 The histological review and the correlation the tumor size and survival time of hMB post-transplanted (p/t) mice: **a** The tumor section of eighth week p/t (*arrows*). **b** Tumor section of 12th week p/t (*arrow*). **c** Growth curve of brain tumor size in p/t mice (n=12). **d** Mean survival curve of p/t mice (n=12)

constitutive GFP signals at the living cellular level and in vivo transplanted grafts could be visualized directly and quickly under a specific excitation wavelength for non-invasive, real-time, and in situ observation. Moreover, by using an immunodeficient mouse model, a system physiologically relevant to humans was successfully established for the investigation of tumor growth effects in MB.

In summary, our data support that in vitro GFP imaging is an efficient tool for early detection and long-term monitoring of tumor progression in the mouse model of xenotransplanted hMB cells. Furthermore, the strategies of GFP imaging can permit a wide variety of molecular biological research in living cells and animals, and will also provide high-throughput in vivo screens that are likely to be more predictive of the target response and the effects of new drugs and biotechnology products in preclinical trials.

Acknowledgements This study was supported by Stem Cell Project (94-396-4/5/6) of Taipei Veterans General Hospital, the Joint Projects of UTVGH (94P1-04/06/10), Yen-Tjing Ling Medical Foundation, and Molecular & Genetic Imaging Core/National Research Program for Genomic Research (NSC91-3112-P-075-001-Y).

References

1. Halperin EC, Constine LS, Tarbell NJ, Kun LE (2005) Pediatric radiation oncology. Lippincott Williams & Wilkins, Philadelphia, pp 89–107
2. McNeil DE, Cote TR, Clegg L, Rorke LB (2002) Incidence and trends in pediatric malignancies medulloblastoma/primitive neuroectodermal tumor: a SEER update. Med Pediatr Oncol 39:190–194
3. Zeltzer PM, Boyett JM, Finlay JL, Albright AL, Rorke LB, Milstein JM (1999) Metastasis stage, adjunvant treatment, and residual tumor are prognostic factors for medulloblastoma in children. J Clin Oncol 17:832–845
4. Rutkowski S, Bode U, Deinlein F, Ottensmeier H, Warmuth-Metz M (2005) Treatment of early childhood medulloblastoma by postoperative chemotherapy alone. N Engl J Med 352:978–986
5. Rice JM (2004) Causation of nervous system tumors in children: insights from traditional and genetically engineered animal models. Toxicol Appl Pharm 199:175–191
6. Dyer MA (2004) Mouse models of childhood cancer of the nervous system. J Clin Pathol 57:561–576
7. Sterling-Levis K, White L (2003) The role of xenografting in pediatric brain tumor research with specific emphasis on medulloblastoma/primitive neuroectodermal tumors of childhood. In Vivo 17:329–342
8. White L, Sterling-Levis K, Kees UR (2001) Medulloblastoma/primitive neuroectodermal tumor studied as a Matrigel enhanced subcutaneous xenograft model. J Clin Neurosci 8:151–156
9. Huang P, Allam A, Taghian A, Freeman J, Duffy M (1995) Growth and metastatic behavior of five human glioblastomas compared with nine other histological types of human tumor xenografts in SCID mice. J Neurosurg 83:308–315
10. Kao CL, Chiou SH, Chen YJ, Singh S, Lin HT (2005) Increased expression of osteopontin gene in atypical teratoid/rhabdoid tumor of the central nervous system. Mod Pathol 18:769–778
11. Chen YJ, Chen PJ, Lee MC, Yeh SH, Hsu MT, Lin CH (2002) Chromosomal analysis of hepatic adenoma and focal nodular hyperplasia by comparative genomic hybridization. Genes Chromosomes Cancer 35:138–143
12. Peng H, Chen ST, Wergedal JE, Polo JM, Yee JK (2001) Development of an MFG-based retroviral vector system for secretion of high levels of functionally active human BMP4. Mol Ther 4:95–104
13. Vachon P, Girard C, Theoret Y (2004) Effects of basic fibroblastic growth factor on the growth of human medulloblastoma xenograft. J Neurooncol 67:139–146
14. Ho DM, Hsu CY, Chiang H (2002) Histopathologic grading of medulloblastomas. Cancer 95:2577–2578
15. Tong CY, Hui AB, Yin XL, Pang JC, Zhu XL (2004) Detection of oncogene amplifications in medulloblastomas by comparative genomic hybridization and array-CGH. J Neurosurg 100:187–193
16. Saunders DE, Hayward RD, Phipps KP, Chong WK, Wade AM (2003) Surveillance neuroimaging of intracranial medulloblastoma in children: how effective, how often, and for how long? J Neurosurg 99:280–286
17. Wetmore C, Eberhart DE, Curran T (2001) Loss of p53 but not accelerate medulloblastoma in mice heterozygous for patched. Cancer Res 61:513–516
18. Pang JC, Chang Q, Chung YF, Teo JG, Poon WS (2005) Epigenetic inactivation of DLC-1 in supratentorial primitive neuroectodermal tumor. Hum Pathol 36:36–43
19. Di Marcotullio L, Ferretti E, De Smaele E, Argenti B, Mincione C (2004) REN^{KCTD11} is a suppressor of hedgehog signaling and is deleted in human medulloblastoma. Proc Natl Acad Sci USA 101:10833–10838
20. Pinte S, Stankovic-Valentin N, Deltour S, Rood BR, Guerardel C, Leprince D (2004) The tumor suppressor gene HIC1 is a sequence-specific transcriptional repressor: definition of its consensus binding sequence and analysis of its DNA binding and repressive properties. J Biol Chem 279: 38313–38324
21. MacDonald TJ, Brown KM, LaFleur B, Peterson K, Lawlor C (2001) Expression profiling of medulloblastoma: PDGFRA and the RAS/MAPK pathway as therapeutic targets for metastatic disease. Nat Genet 29:143–152
22. Gilbertson RJ, Clifford SC (2003) PDGFRB is overexpressed in metastatic medulloblastoma. Nat Genet 35:197–198
23. Cubitt AB, Heim R, Adams SR, Boyd AE, Gross LA, Tsien RY (1995) Understanding, improving and using green fluorescent proteins. Trends Biochem Sci 20:448–455
24. Niwa H, Inouye S, Hirano T, Matsuno T, Kojima S (1996) Chemical nature of the light emitter of the *Aequorea* green fluorescent protein. Proc Natl Acad Sci USA 93:13617–13622
25. Hanson MR, Kohler RH (2001) GFP imaging: methodology and application to investigate cellular compartmentation in plants. J Exp Bot 52:529–539
26. Alba FJ, Bermudez A, Daban JR (2001) Green-light transilluminator for the detection without photodamage of proteins and DNA labeled with different fluorescent dyes. Electrophoresis 22:399–403
27. Jing D, Agnew J, Patton WF, Hendrickson J, Beechem JM (2003) A sensitive two-color electrophoretic mobility shift assay for detecting both nucleic acids and protein in gels. Proteomics 3:1172–1180